Applied Physics Letters

Towards generation of millihertz-linewidth laser light with 10^{-18} frequency instability via four-wave mixing

Cite as: Appl. Phys. Lett. **114**, 051104 (2019); https://doi.org/10.1063/1.5082660
Submitted: 22 November 2018 . Accepted: 20 January 2019 . Published Online: 07 February 2019

Li Jin, Chao Hang, Yanyi Jiang, Chengjie Zhu, Zhan Zheng, Yuan Yao, Guoxiang Huang, and Longsheng Ma

Applied Physics Letters ARTICLE scitation.org/journal/apl

Towards generation of millihertz-linewidth laser light with 10^{-18} frequency instability via four-wave mixing

Cite as: Appl. Phys. Lett. **114**, 051104 (2019); doi: 10.1063/1.5082660
Submitted: 22 November 2018 · Accepted: 20 January 2019 ·
Published Online: 7 February 2019

View Online Export Citation CrossMark

Li Jin,[1] Chao Hang,[1] Yanyi Jiang,[1,2,a)] Chengjie Zhu,[3,a)] Zhan Zheng,[4] Yuan Yao,[1] Guoxiang Huang,[1,2] and Longsheng Ma[1,2]

AFFILIATIONS

[1] State Key Laboratory of Precision Spectroscopy, East China Normal University, Shanghai 200062, China
[2] Collaborative Innovation Center of Extreme Optics, Shanxi University, Taiyuan 030006, China
[3] MOE Key Laboratory of Advanced Micro-Structured Materials, School of Physics Science and Engineering, Tongji University, Shanghai 200092, China
[4] Center for Optics and Optoelectronics Research (COOR), Collaborative Innovation Center for Information Technology in Biological and Medical Physics, College of Science, Zhejiang University of Technology, Hangzhou 310023, China

[a)] Authors to whom correspondence should be addressed: yyjiang@phy.ecnu.edu.cn and cjzhu@tongji.edu.cn

ABSTRACT

Laser light with spectral purity and frequency stability is pursued in precision spectroscopy and precision measurements. We propose a scheme to generate millihertz-linewidth laser light with a frequency instability of 10^{-18} via optical four-wave mixing in alkaline-earth atoms. We show that the linewidth of the mixing laser light is ultimately limited by the natural linewidth of the atomic transition rather than by the linewidth of the input lasers. The frequency stability of the mixing laser light depends largely on the intensity stability of the input lasers. It is possible to generate a millihertz-linewidth laser light with a frequency instability of 10^{-18} and a power of 10^{-12} W when the input lasers with a relative intensity instability of 10^{-4} and a spectral width of 1 Hz interact with strontium (Sr) atoms with a density of $1 \times 10^{11}\,\mathrm{cm}^{-3}$.

Profiting from long coherence time and low phase noise, lasers with high frequency stability and narrow linewidth are central to many applications, such as gravitational wave detection, optical atomic clock, low phase-noise microwave generation, optical frequency synthesizer, and quantum computation.[1–6] Most of the state-of-the-art ultra-stable lasers have been realized by stabilizing their frequencies to the resonance of stable optical reference cavities.[7–9] Thermal noise of the optical reference cavities is the ultimate limitation on the frequency stability of cavity-stabilized lasers.[10] Strength has been exerted to reduce the cavity thermal noise by increasing the cavity length,[8,11–14] reducing the temperature of cavities,[9,15] or using low mechanical loss materials for mirror substrates and coating.[16] By combining some of those methods, laser frequency instability at an averaging time of 1 s has been pushed from 10^{-15} to 10^{-17}, and the laser linewidth improved from 1 Hz to 10 mHz.[9]

However, the pursuit of generation of laser light with even better frequency stability has never stopped. Taking optical atomic clocks as an example, when the frequency instability of a narrow-linewidth laser as a local oscillator is reduced from 10^{-15} to 10^{-16}, the frequency instability of an optical clock is improved from $10^{-15}/\sqrt{\tau}$ to $10^{-16}/\sqrt{\tau}$ (τ is the averaging time),[11–13] enabling 10^{-18} frequency precision in an averaging time of less than one day. Further improvement on ultra-stable lasers will speed up the measurement time using optical atomic clocks and will open up new applications in sub-mm very long baseline interferometry,[17] atom interferometry,[18] deep space navigation,[19] and geodesy.[20,21]

Alternative ways have been investigated in parallel to circumvent the cavity thermal noise. The phase-matching effect of the non-adiabatic interaction of two quasi-monochromatic fields with Sr atoms provides a possible way to realize a difference-frequency-generation-based laser with an expected linewidth of 2 mHz.[22] One another approach is to stabilize the laser frequency to a narrow-linewidth atomic transition such as the clock transitions of alkaline-earth atoms used for optical atomic clocks, which provides a high-resolution laser frequency discrimination signal.[23,24] Meanwhile, cavity-enhanced spectroscopy is employed to compensate the weak interaction with those transitions. In the method of active optical clocks, narrow-linewidth laser light can be directly generated in a bad cavity or superradiant regime,[25–27] where the frequency of the emitted laser light is mainly set by the narrow spectral transition of gain medium rather than the cavity length. A laser frequency instability of 6.7×10^{-16} at 1 s was recently demonstrated.[27]

In this letter, we propose a scheme for the generation of millihertz-linewidth laser light with high frequency stability based on four-wave mixing (FWM) in atoms with an ultra-narrow-linewidth transition, e.g., the clock transitions of alkaline-earth atoms. Due to energy conservation, the frequency of the mixing laser is set by the sum of the frequencies of the input lasers. However, the generation efficiency of FWM is determined by the narrow-linewidth atomic system, serving as a filter to let the mixing laser with a narrow spectrum pass through. Any frequency fluctuation on the input lasers is converted into amplitude fluctuation on the mixing light. The spectral purity of the mixing laser or the filter bandwidth of the atomic system can be adjusted by varying the intensity and the frequency detuning of the input lasers. It can ultimately approach the natural linewidth of the extremely weak dipole transition of alkaline-earth atoms at the millihertz level, even if the linewidth of the input lasers is at the hertz level. The frequency stability of the mixing laser is found to be sensitive to the intensity stability of the input lasers. With 10^{-4} relative intensity instability and 1 Hz spectral width of input lasers, taking Sr atoms with a density of $1 \times 10^{11}\,\mathrm{cm}^{-3}$ as an example, the mixing laser light is expected to have a linewidth of 4 mHz, a frequency instability of 10^{-18}, and a power of 10^{-12} W, which is sufficient to phase-lock a slave laser with high power to inherit the phase coherence of the mixing laser.[28]

The proposed scheme consists of a four-level atomic system interacting with three coherent laser fields E_j with angular frequencies of ω_j ($j = 1, 2, 3$). To reduce the phase excursion of the input lasers, their frequencies can be stabilized to an optical frequency comb, which is phase-locked to a cavity-stabilized laser,[29,30] as shown in Fig. 1(a). The laser fields of E_1, E_2, and E_3 couple the transitions between $|1\rangle \leftrightarrow |2\rangle$, $|2\rangle \leftrightarrow |3\rangle$, and $|3\rangle \leftrightarrow |4\rangle$, respectively. The related energy levels are shown in Fig. 1(b). The generated laser field, referred to as the mixing field E_m, satisfies the momentum conservation relation $k_m = k_1 + k_2 - k_3$ and the energy conservation relation $\omega_m = \omega_1 + \omega_2 - \omega_3$ (k_j is the wave vector and ω_m is the angular frequency of the mixing field). Here, we consider an ensemble of N atoms confined in optical lattice sites, where the Doppler broadening and the recoil effect can be neglected. The wavelength of the lattice laser is set to the magic wavelength to cancel out the Stark shift between the energy levels of $|4\rangle$ and $|1\rangle$. Three input laser fields propagate along the optical lattice light.

Driven by the laser fields, the evolution of atomic coherence can be described by the following density matrix equation:

$$\frac{d}{dt}\sigma(t) = -\frac{i}{\hbar}[H, \sigma(t)] + \mathcal{L}[\sigma(t)], \tag{1}$$

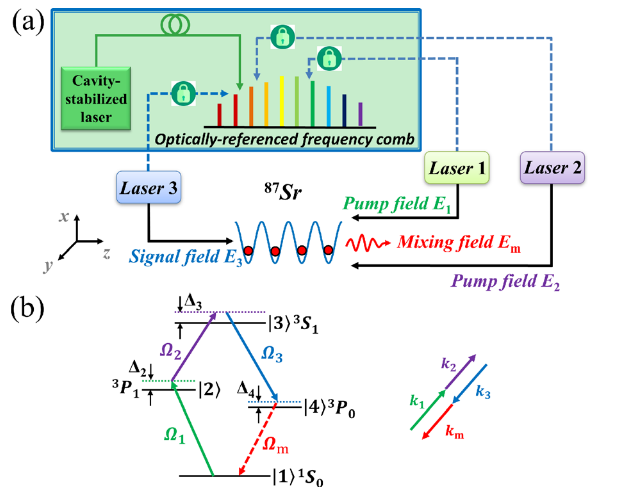

FIG. 1. (a) Experimental diagram of FWM in a four-level atomic system in optical lattice sites. (b) The related energy-level for the FWM scheme.

where $\sigma(t)$ is the time-dependent atomic density matrix. The Hamiltonian under the rotating-wave approximation is given by

$$H = \hbar \begin{pmatrix} 0 & -\Omega_1^* & 0 & -\Omega_m^* \\ -\Omega_1 & -\Delta_2 & -\Omega_2^* & 0 \\ 0 & -\Omega_2 & -\Delta_3 & -\Omega_3 \\ -\Omega_m & 0 & -\Omega_3^* & -\Delta_4 \end{pmatrix}, \tag{2}$$

where Ω_j ($j = 1, 2, 3, m$) $= \wp_{kl} E_j/\hbar$ is the Rabi frequency of the relevant atomic transition in a given laser field E_j, $\wp_{kl}$ [the subscripts $k, l = 1-4$ refer to the four energy levels illustrated in Fig. 1(b) $k \neq l$] is the dipole matrix element between the relevant states, $\Delta_2 = \omega_1 - \omega_{21}$, $\Delta_3 = \omega_1 + \omega_2 - \omega_{31}$, and $\Delta_4 = \omega_1 + \omega_2 - \omega_3 - \omega_{41}$ (ω_{kl} is the angular frequency of atomic transitions. The Liouville matrix $\mathcal{L}[\sigma(t)]$ in Eq. (1) describes atomic decoherence due to spontaneous emission, given by

$$\mathcal{L}[\sigma(t)] = \begin{pmatrix} \mathcal{L}_{11} & -\gamma_{12}\sigma_{12} & -\gamma_{13}\sigma_{13} & -\gamma_{14}\sigma_{14} \\ -\gamma_{21}\sigma_{21} & \mathcal{L}_{22} & -\gamma_{23}\sigma_{23} & -\gamma_{24}\sigma_{24} \\ -\gamma_{31}\sigma_{31} & -\gamma_{32}\sigma_{32} & \mathcal{L}_{33} & -\gamma_{34}\sigma_{34} \\ -\gamma_{41}\sigma_{41} & -\gamma_{42}\sigma_{42} & -\gamma_{43}\sigma_{43} & \mathcal{L}_{44} \end{pmatrix}, \tag{3}$$

where $\mathcal{L}_{11} = \Gamma_{21}\sigma_{22} + \Gamma_{41}\sigma_{44}$, $\mathcal{L}_{22} = -\Gamma_{21}\sigma_{22} + \Gamma_{32}\sigma_{33}$, $\mathcal{L}_{33} = -(\Gamma_{32} + \Gamma_{34})\sigma_{33}$, $\mathcal{L}_{44} = -\Gamma_{41}\sigma_{44} + \Gamma_{34}\sigma_{33}$, and Γ_{kl} and γ_{kl} are the population and coherence decay rates, respectively. Since the atoms are confined in optical lattice sites, the coherence decay due to atomic collision is negligible. The coherence decay rate is $\gamma_{kl} = (\Gamma_k + \Gamma_l)/2$, where Γ_k and Γ_l denote the total decay rates of energy levels $|k\rangle$ and $|l\rangle$, respectively.

Under the slowly varying amplitude approximation, the following Maxwell equations describe the propagation of the signal field E_3 and the generation of the mixing laser field E_m:

$$i\left(\frac{\partial}{\partial z} + \frac{1}{c}\frac{\partial}{\partial t}\right)\Omega_3 + \kappa_{34}\sigma_{34} = 0, \tag{4a}$$

$$i\left(\frac{\partial}{\partial z}+\frac{1}{c}\frac{\partial}{\partial t}\right)\Omega_m+\kappa_{41}\sigma_{41}=0, \tag{4b}$$

where $\kappa_{34,41}=\omega_{3,m}|\wp_{34,41}|^2N_a/(2\hbar\varepsilon_0 c)$, with N_a being the atomic density. Since most atoms are populated in the ground state $|1\rangle$, one could assume $\sigma_{11}\approx 1$. The Fourier transformation of the related Maxwell-Bloch Eqs. (1) and (4) is given by

$$(\omega+d_{41})\tilde{\sigma}_{41}+\Lambda_m-\Lambda_1\tilde{\sigma}_{42}+\Lambda_3^*\tilde{\sigma}_{31}=0, \tag{5a}$$

$$d_{42}\tilde{\sigma}_{42}+\Lambda_3^*\tilde{\sigma}_{32}-\Lambda_1^*\tilde{\sigma}_{41}-\Lambda_2\tilde{\sigma}_{43}=0, \tag{5b}$$

$$d_{43}\tilde{\sigma}_{43}-\Lambda_2^*\tilde{\sigma}_{42}=0, \tag{5c}$$

$$-i\frac{\partial}{\partial z}\Lambda_3^*-\frac{\omega}{c}\Lambda_3^*+\kappa_{43}\tilde{\sigma}_{43}=0, \tag{5d}$$

$$i\frac{\partial}{\partial z}\Lambda_m+\frac{\omega}{c}\Lambda_m+\kappa_{41}\tilde{\sigma}_{41}=0, \tag{5e}$$

where $d_{kl}=\Delta_k-\Delta_l+i\gamma_{kl}$, ω is the Fourier frequency, and $\tilde{\sigma}_{kl}$ and Λ_j are the Fourier transformations of σ_{kl} and Ω_j, respectively. In deriving Eqs. (5), we have treated σ_{kl} adiabatically except σ_{41} since the decoherence rate γ_{41} is much smaller than the other decay rates. The solutions of (5d) and (5e), $\Lambda_3(z,\omega)$ and $\Lambda_m(z,\omega)$, indicate the dynamic evolution of the signal field and generation of the mixing field in the frequency domain.

By substituting Eqs. (5a)–(5c) into Eqs. (5d) and (5e), we obtain

$$i\frac{\partial}{\partial z}\Lambda_3^*+\left(\frac{\omega}{c}+\frac{\kappa_{43}|D_0|^2}{\omega+d}\right)\Lambda_3^*+\frac{\kappa_{43}D_0^*}{(\omega+d)}\Lambda_m=0, \tag{6a}$$

$$i\frac{\partial}{\partial z}\Lambda_m+\left(\frac{\omega}{c}-\frac{\kappa_{41}}{\omega+d}\right)\Lambda_m-\frac{\kappa_{41}D_0}{(\omega+d)}\Lambda_3^*=0, \tag{6b}$$

where $D_0=\Lambda_1\Lambda_2/(d_{21}d_{31}-|\Lambda_2|^2)$ and $d=d_{41}+d_{21}|\Lambda_3|^2/(|\Lambda_2|^2-d_{21}d_{31})+d_{43}|\Lambda_1|^2/(|\Lambda_2|^2-d_{42}d_{43})$. For a given initial condition of $\Lambda_m(z=0,\omega)=0$, one can get the analytical solutions as follows:

$$\Lambda_3^*(z,\omega)=\frac{\kappa_{41}\Lambda_3^*}{\kappa_{41}-\kappa_{43}|D_0|^2}\exp\left(\frac{i\omega z}{c}\right)-\frac{\kappa_{43}|D_0|^2\Lambda_3^*}{\kappa_{41}-\kappa_{43}|D_0|^2}\exp\left[i\left(\frac{\omega}{c}-\frac{\kappa_{41}-\kappa_{43}|D_0|^2}{\omega+d}\right)z\right], \tag{7a}$$

$$\Lambda_m(z,\omega)=\frac{\kappa_{41}D_0\Lambda_3^*}{\kappa_{41}-\kappa_{43}|D_0|^2}\times\left\{\exp\left[i\left(\frac{\omega}{c}-\frac{\kappa_{41}-\kappa_{43}|D_0|^2}{\omega+d}\right)z\right]-\exp\left(\frac{i\omega z}{c}\right)\right\}. \tag{7b}$$

Since our parameters satisfy $\left(\kappa_{41}-\kappa_{43}|D_0|^2\right)z\ll \mathrm{Im}[d]$, the term in the brace of Eq. (7b) is approximately $(\kappa_{41}-\kappa_{43}|D_0|^2)z/(\omega+d)$. Therefore, the intensity of the mixing laser is

$$I_m\propto\frac{|\Lambda_1\Lambda_2\Lambda_3^*|^2\kappa_{41}^2z^2}{(\omega+\mathrm{Re}[d])^2+(\mathrm{Im}[d])^2}. \tag{8}$$

It shows that the linewidth of the mixing laser light is determined by the product of $|\Lambda_1\Lambda_2\Lambda_3^*|^2$ and $[(\omega+\mathrm{Re}[d])^2+(\mathrm{Im}[d])^2]^{-1}$. Considering the spectral distribution of the incident lasers, $\Lambda_1\Lambda_2\Lambda_3^*$ can be written as $\Lambda_{10}\Lambda_{20}\Lambda_{30}^*S(\omega)$. Since the spectral width of the input lasers, $|S(\omega)|^2$, can be controlled at the hertz level, which can be larger than $\mathrm{Im}[d]/\pi$, the full width at half maximum (FWHM) linewidth of the mixing laser ($\Delta\nu_{\mathrm{FWHM}}$) is roughly equal to $\mathrm{Im}[d]/\pi$.

When $\Delta_2\gg\Gamma_2$, $\Delta_3\gg\Gamma_3$, $\Delta_2\Delta_3\gg\Lambda_2^2$, and $\Delta_4=0$

$$\mathrm{Im}[d]\sim\frac{1}{2}\left(\Gamma_{41}+\frac{|\Lambda_{30}|^2\Gamma_3}{|\Delta_3|^2}+\frac{|\Lambda_{10}\Lambda_{20}|^2\Gamma_3}{|\Delta_2\Delta_3|^2}+\frac{|\Lambda_{10}|^2\Gamma_2}{|\Delta_2|^2}\right). \tag{9}$$

The first term in Eq. (9), Γ_{41}, represents the spontaneous decay rate of the $|4\rangle$ ($^3P_0$) state, whose linewidth is at the millihertz level for Sr or Yb atoms. Once appropriate intensity and frequency detuning of the input lasers are chosen to satisfy $|\Lambda_{30}|^2\Gamma_3/|\Delta_3|^2+|\Lambda_{10}\Lambda_{20}|^2\Gamma_3/|\Delta_2\Delta_3|^2+|\Lambda_{10}|^2\Gamma_2/|\Delta_2|^2\sim\Gamma_{41}$, $\mathrm{Im}[d]$ will be close to Γ_{41}.

For experimental considerations, we take ^{87}Sr atoms as an example, which are trapped and cooled first on the strong $^1S_0\to{}^1P_1$ transition and second on the narrower $^1S_0\to{}^3P_1$ transition. The atoms are then loaded into optical lattice sites with an atomic density N_a of $1\times10^{11}\,\mathrm{cm}^{-3}$. In order to generate a continuous mixing laser, it might be better to have continuous atom-loading by preparing laser-cooled atoms right above the optical lattice and then loading into optical lattice sites with either gravity or optical conveyor.[31] The energy levels $|2\rangle$ and $|3\rangle$ are the states of $^3P_1$ and $^3S_1$, respectively. The laser wavelengths of E_1, E_2, and E_3 are 689 nm, 688 nm, and 679 nm, respectively. The electric dipole moments $\wp_{34}$ and $\wp_{41}$ are 16.2×10^{-30} C·m and 2.8×10^{-34} C·m, respectively.[32]

According to Eq. (8), in order to obtain a mixing laser light with a linewidth of a few millihertz, we choose $\Lambda_{10}/(2\pi)=20$ kHz (corresponding to light power of $P_1=6.1\,\mu$W when the beam radius is 500 μm for E_j), $\Lambda_{20}/(2\pi)=31.8$ MHz ($P_2=29.8$ mW), and $\Lambda_{30}^*/(2\pi)=10$ kHz ($P_3=8.6$ nW). The spectral distribution of the input laser fields is chosen as $|S(\omega)|^2=\exp[-\omega^2/(2\pi^2/\mathrm{In}2)]$, corresponding to a spectral width of 1 Hz. The frequency detuning of the input lasers is chosen as $\Delta_{2,3,4}/(2\pi)=-64.6$ MHz, -1.36 GHz, and 0 Hz, respectively. Figures 2(a) and 2(b) show the spectrum of the mixing laser and the signal laser versus propagation distance z. The mixing laser grows rapidly during the propagation. Its spectrum is a Lorentzian profile with a linewidth of 4 mHz. The atomic system allows the mixing field with an angular frequency satisfying $|\omega_m-\omega_{41}|<2\mathrm{Im}[d]$ to generate efficiently. Figure 2(b) shows that E_3 preserves its Gaussian profile during the propagation except for an additional peak at its central frequency.

To make a comparison with the above analytical solution, we numerically solve Eqs. (1) and (4). The time evolution of the atomic density matrix is performed by using an adaptive Runge-Kutta algorithm, and the propagation of the conjugated laser fields is carried out by using the Lax-Wendroff finite-difference method. We made numerical simulation with the same 1-Hz-linewidth input lasers by considering a temporal distribution $|S(t)|^2=\sqrt{\pi/(2\mathrm{In}2)}\exp[-t^2/(2\mathrm{In}2/\pi^2)]$. The solid lines in Figs. 2(c) and 2(d) are the spectrum of the mixing laser and the signal laser at $z=0.13$ mm based on the simulation results, which are close to the analytical results (dashed line).

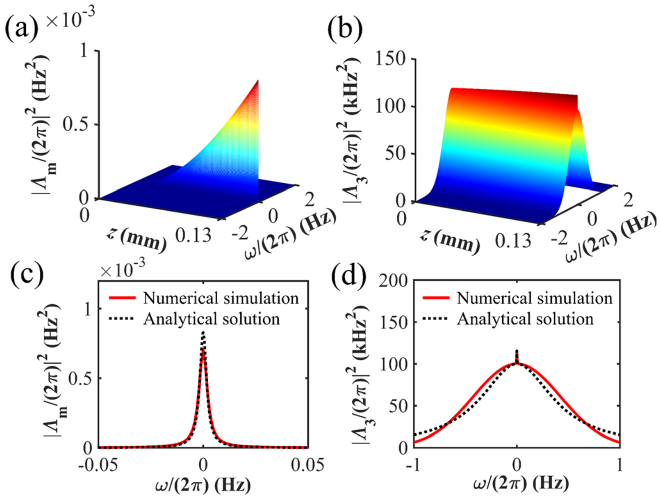

FIG. 2. The dynamic evolution of the conjugated laser fields in the four-wave mixing process. The generation of the mixing field (a) and the propagation of the signal field (b) versus propagation distance z. The spectra of the mixing and the signal fields are shown in (c) and (d) at $z = 0.13$ mm, respectively. The black dashed line and the red solid line represent the analytical solution and the numerical simulation, respectively.

The frequency stability of the mixing laser is dependent on the Stark shift of the transition $|1\rangle \leftrightarrow |4\rangle$, which is determined by the real part of d

$$\mathrm{Re}[d] \sim \frac{|\Lambda_{10}|^2}{\Delta_2} - \frac{|\Lambda_{30}|^2}{\Delta_3}. \tag{10}$$

It shows that the frequency or intensity variations of the input lasers result in the variation of Re[d]. The fractional frequency instability of the mixing laser can be written as $\sigma_f = \mathrm{Re}[d] \times (\xi_I + \xi_f)/\omega_m$, where ξ_I and ξ_f represent the fractional intensity instability and the fractional frequency instability of the input lasers, respectively. By phase-locking the input lasers to a frequency-stabilized optical frequency comb, ξ_f can be controlled on the order of 10^{-15} at an averaging time of 1 s.[33] Although the frequency of the lattice light is set to the magic wavelength for $|1\rangle \leftrightarrow |4\rangle$, it is not magic for the other transitions involved. Thus, the intensity fluctuation of the lattice light changes Δ_2 and Δ_3. When the intensity fluctuation of the lattice light is controlled within 4%, $\xi_f = 1 \times 10^{-4}$. The relative intensity fluctuation ξ_I can be experimentally controlled better than 10^{-3} in most cases and ultimately 10^{-5} at an averaging time of 1 s.[5,16] Taking case (d) in Table I as an example, Re[d]/(2π) can be −6.2 Hz. When $\xi_I = 10^{-4}$, the fractional frequency instability σ_f of the mixing laser is 2×10^{-18} at an averaging time of 1 s.

When considering the contributions of all higher lying states that are coupled to $|1\rangle$ and $|4\rangle$ [not shown in Fig. 1(b)], the net stark shift of $|1\rangle \rightarrow |4\rangle$ transition of Sr atoms induced by the input lasers is −5.75 Hz when using the same parameters as those for case (d) in Table I. The frequency instability of the mixing laser light will be 2.6×10^{-18} when ξ_I is 10^{-4}.

While the frequency instability of E_j does not affect the frequency instability of the mixing laser light, it does affect its intensity. When ξ_f is 1×10^{-15} (or 5×10^{-16}), the fractional intensity instability of the mixing laser is 13% (or 3.3%), according to Eq. (8) with the attenuated spectrum amplitude of E_j.

As shown in Table I, the linewidth of the mixing laser can be adjusted from the hertz level to the millihertz level while its frequency instability can be adjusted from 10^{-15} to 10^{-18} by varying the intensity and the frequency detuning of the incident laser fields. The power of the mixing laser is obtained by calculating the power spectral density (PSD) of the mixing field with the Wiener-Khintchine theorem[34] and integrating the PSD. The spectral width of the input lasers is 1 Hz. The intensity instability of E_j is $\xi_I = 10^{-4}$ for cases (a)–(d), while $\xi_I = 10^{-5}$ for case (e). If ξ_I is 10^{-5}, the power of the mixing laser can be an order of magnitude higher, as shown in cases (d) and (e).

Equation (7b) also allows us to determine the peak Rabi frequency of the mixing laser. Figure 3 shows the dependence of the peak Rabi frequency of the mixing field on the atomic density N_a at different propagation distances z. For weak coherent propagation, e.g., a short propagation distance or low atomic density, $\Lambda_{m0} \propto \kappa_{41} z \propto N_a z$. While for strong coherent propagation, the output intensity reaches its maximum of $\Lambda^s_{m0} = \kappa_{41}\Lambda_{10}\Lambda_{20}\Lambda_{30}/[(\kappa_{41} - \kappa_{43}|D_0|^2)(d_{21}d_{31} - |\Lambda_{20}|^2)]$, when multiphoton destructive interference becomes effective.[35] For the same values of the input laser fields as those used in Fig. 2, $|\Lambda_{m0}|/(2\pi)$ reaches its maximum of 0.09 Hz when the atomic density is 2×10^{12} cm^{-3} at the propagation distance $z = 130\ \mu$m.

In the proposed FWM scheme, the linewidth of the mixing laser light is ultimately limited by the natural linewidth of the

TABLE I. The detuning and Rabi frequency of the incident laser fields for generating the mixing laser light with different linewidths and frequency instabilities. The power of the mixing laser is calculated with the Wiener-Khintchine theorem and integrating the PSD, with an atomic diameter of 100 μm. The spectral width of the input lasers is 1 Hz. The intensity instability is $\xi_I = 10^{-4}$ for cases (a)–(d), while $\xi_I = 10^{-5}$ for case (e). The atomic density $N_a = 3 \times 10^{11}$ cm^{-3} for cases (a)–(c), while $N_a = 1 \times 10^{11}$ cm^{-3} for cases (d) and (e) due to saturation broadening.

						The mixing laser			
	$\Lambda_{10}/(2\pi)$ (MHz)	$\Lambda_{20}/(2\pi)$ (MHz)	$\Lambda_{30}/(2\pi)$ (MHz)	$\Delta_2/(2\pi)$ (MHz)	$\Delta_3/(2\pi)$ (GHz)	$\Delta\nu_{FWHM}$ (mHz)	σ_f	$|\Lambda_{m0}|/(2\pi)$ (Hz)	Power (pW)
a	0.65	31.8	0.21	96.6	1.36	600	1×10^{-15}	0.19	6700
b	0.21	31.8	0.067	97.5	1.36	90	1×10^{-16}	0.18	1296
c	0.068	31.8	0.02	107.2	1.36	10	1×10^{-17}	0.13	96
d	0.02	31.8	0.01	64.6	1.36	4	2×10^{-18}	0.03	1.6
e	0.29	95.5	0.028	0.96	4	4	2×10^{-18}	0.095	16

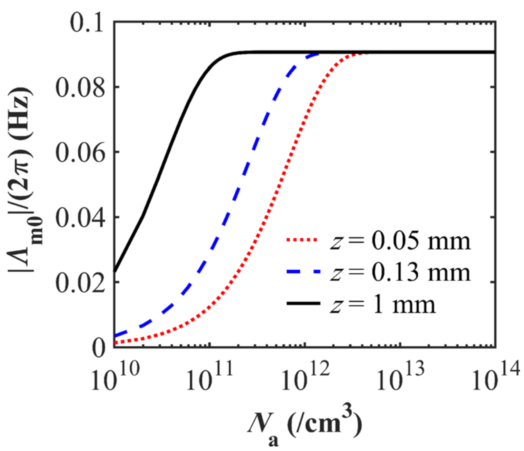

FIG. 3. The peak Rabi frequency of the mixing field $|\Lambda_{m0}|/(2\pi)$ as a function of atomic density N_a at different propagation distances z.

atomic transition rather than the linewidth of the input lasers. The frequency stability of the mixing laser depends largely on the intensity stability of the input lasers and the lattice light. It is possible to obtain the mixing laser with a frequency instability of 2×10^{-18}, a spectral width of 4 mHz, and an output power of 10^{-12} W if input lasers with an intensity instability of 10^{-4} and a spectral width of 1 Hz interact with Sr atoms with a density of $1\times10^{11}\,\mathrm{cm}^{-3}$. This mechanism may open an avenue for generating millihertz-linewidth laser light with superior frequency stability.

This work was supported by the National Natural Science Foundation of China (91636214, 11822402, 11654004, 11604297, 11475063, and 11474099), the National Key R&D Program of China (2017YFA0304403, 2016YFA0302103, and 2017YFA0304201), and the 111 Project (B12024).

REFERENCES

[1]R. X. Adhikari, Rev. Mod. Phys. **86**, 121 (2014).
[2]A. D. Ludlow, M. M. Boyd, J. Ye, E. Peik, and P. O. Schmidt, Rev. Mod. Phys. **87**, 637 (2015).
[3]T. L. Nicholson, S. L. Campbell, R. B. Hutson, G. E. Marti, B. J. Bloom, R. L. McNally, W. Zhang, M. D. Barrett, M. S. Safronova, G. F. Strouse, W. L. Tew, and J. Ye, Nat. Commun. **6**, 6896 (2015).
[4]T. M. Fortier, M. S. Kirchner, F. Quinlan, J. Taylor, J. C. Bergquist, T. Rosenband, N. Lemke, A. Ludlow, Y. Jiang, C. W. Oates, and S. A. Diddams, Nat. Photonics **5**, 425 (2011).
[5]Y. Yao, Y. Y. Jiang, L. F. Wu, H. F. Yu, Z. Y. Bi, and L. S. Ma, Appl. Phys. Lett. **109**, 131102 (2016).
[6]D. Leibfried, R. Blatt, C. Monroe, and D. Wineland, Rev. Mod. Phys. **75**, 281 (2003).
[7]B. C. Young, F. C. Cruz, W. M. Itano, and J. C. Bergquist, Phys. Rev. Lett. **82**, 3799 (1999).
[8]S. Häfner, S. Falke, C. Grebing, S. Vogt, T. Legero, M. Merimaa, C. Lisdat, and U. Sterr, Opt. Lett. **40**, 2112 (2015).
[9]D. G. Matei, T. Legero, S. Häfner, C. Grebing, R. Weyrich, W. Zhang, L. Sonderhouse, J. M. Robinson, J. Ye, F. Riehle, and U. Sterr, Phys. Rev. Lett. **118**, 263202 (2017).
[10]K. Numata, A. Kemery, and J. Camp, Phys. Rev. Lett. **93**, 250602 (2004).
[11]Y. Y. Jiang, A. D. Ludlow, N. D. Lemke, R. W. Fox, J. A. Sherman, L.-S. Ma, and C. W. Oates, Nat. Photonics **5**, 158 (2011).
[12]T. L. Nicholson, M. J. Martin, J. R. Williams, B. J. Bloom, M. Bishof, M. D. Swallows, S. L. Campbell, and J. Ye, Phys. Rev. Lett. **109**, 230801 (2012).
[13]N. Nemitz, T. Ohkubo, M. Takamoto, I. Ushijima, M. Das, N. Ohmae, and H. Katori, Nat. Photonics **10**, 258 (2016).
[14]L. Jin, Y. Y. Jiang, Y. Yao, H. F. Yu, Z. Y. Bi, and L. S. Ma, Opt. Express **26**, 18699 (2018).
[15]W. Zhang, J. M. Robinson, L. Sonderhouse, E. Oelker, C. Benko, J. L. Hall, T. Legero, D. G. Matei, F. Riehle, U. Sterr, and J. Ye, Phys. Rev. Lett. **119**, 243601 (2017).
[16]G. D. Cole, W. Zhang, M. J. Martin, J. Ye, and M. Aspelmeyer, Nat. Photonics **7**, 644 (2013).
[17]S. Doeleman, T. Mai, A. E. E. Rogers, J. G. Hartnett, M. E. Tobar, and N. Nand, Publ. Astron. Soc. Pac. **123**, 582 (2011).
[18]J. M. Hogan and M. A. Kasevich, Phys. Rev. A **94**, 033632 (2016).
[19]S. Grop, P. Y. Bourgeois, N. Bazin, Y. Kersalé, E. Rubiola, C. Langham, M. Oxborrow, D. Clapton, S. Walker, J. De Vicente, and V. Giordano, Rev. Sci. Instrum. **81**, 025102 (2010).
[20]T. Takano, M. Takamoto, I. Ushijima, N. Ohmae, T. Akatsuka, A. Yamaguchi, Y. Kuroishi, H. Munekane, B. Miyahara, and H. Katori, Nat. Photonics **10**, 662 (2016).
[21]J. Grotti, S. Koller, S. Vogt, S. Häfner, U. Sterr, C. Lisdat, H. Denker, C. Voigt, L. Timmen, A. Rolland, F. N. Baynes, H. S. Margolis, M. Zampaolo, P. Thoumany, M. Pizzocaro, B. Rauf, F. Bregolin, A. Tampellini, P. Barbieri, M. Zucco, G. A. Costanzo, C. Clivati, F. Levi, and D. Calonico, Nat. Phys. **14**, 437 (2018).
[22]D. Yu and J. Chen, Phys. Rev. Lett. **98**, 050801 (2007).
[23]P. G. Westergaard, B. T. R. Christensen, D. Tieri, R. Matin, J. Cooper, M. Holland, J. Ye, and J. W. Thomsen, Phys. Rev. Lett. **114**, 093002 (2015).
[24]D. A. Tieri, J. Cooper, B. T. R. Christensen, J. W. Thomsen, and M. J. Holland, Phys. Rev. A **92**, 013817 (2015).
[25]D. Meiser, J. Ye, D. R. Carlson, and M. J. Holland, Phys. Rev. Lett. **102**, 163601 (2009).
[26]M. A. Norcia, M. N. Winchester, J. R. K. Cline, and J. K. Thompson, Sci. Adv. **2**, e1601231 (2016).
[27]M. A. Norcia, J. R. K. Cline, J. A. Muniz, J. M. Robinson, R. B. Hutson, A. Goban, G. E. Marti, J. Ye, and J. K. Thompson, Phys. Rev. X **8**, 021036 (2018).
[28]S. P. Francis, T. T.-Y. Lam, K. McKenzie, A. J. Sutton, R. L. Ward, D. E. McClelland, and D. A. Shaddock, Opt. Lett. **39**, 5251 (2014).
[29]S. Fang, H. Q. Chen, T. Y. Wang, Y. Y. Jiang, Z. Y. Bi, and L. S. Ma, Appl. Phys. Lett. **102**, 231118 (2013).
[30]Y. Yao, Y. Jiang, H. Yu, Z. Bi, and L. Ma, Natl. Sci. Rev. **3**, 463 (2016).
[31]G. A. Kazakov and T. Schumm, in *Proceedings of the European Frequency and Time Conference*, Neuchâtel, Switzerland, 23–26 June 2014 (IEEE, New York City, 2014), pp. 411-414.
[32]M. S. Safronova, S. G. Porsev, U. I. Safronova, M. G. Kozlov, and C. W. Clark, Phys. Rev. A **87**, 012509 (2013).
[33]S. Fang, Y. Y. Jiang, H. Q. Chen, Y. Yao, Z. Y. Bi, and L. S. Ma, Chin. Phys. B **24**, 074202 (2015).
[34]F. Riehle, *Frequency Standards Basics and Applications* (Wiley-VCH Verlag GmbH & Co. KGaA, 2004), p. 57.
[35]L. Deng, M. G. Payne, and W. R. Garrett, Phys. Rep. **429**, 123 (2006).